JOURNAL OF THEORETICAL AND APPLIED MECHANICS
56, 2, pp. 457-469, Warsaw 2018
DOI: 10.15632/jtam-pl.56.2.457

EXPERIMENTAL INVESTIGATION AND MODELLING OF HOT FORMING B_4C/AA6061 LOW VOLUME FRACTION REINFORCEMENT COMPOSITES

Kailun Zheng, **Jianguo Lin**

Imperial College London, Department of Mechanical Engineering, United Kingdom

e-mail: k.zheng13@imperial.ac.uk; jianguo.lin@imperial.ac.uk

Gaohui Wu

Harbin Institute of Technology, School of Material Science and Engineering, Harbin, China

e-mail: wugh@hit.edu.cn

Roger W. Hall

Marbeau Design Consultancy, Paris, France

e-mail: marbeau.dc@sfr.fr

Trevor A. Dean

University of Birmingham, Department of Mechanical Engineering, Birmingham, United Kingdom

e-mail: t.a.dean@bham.ac.uk

This paper presents an experimental investigation of the hot deformation behaviour of 15% B_4C particle reinforced AA6061 matrix composites and the establishment of a novel corresponding unified and physically-based visco-plastic material model. The feasibility of hot forming of a metal matrix composite (MMC) with a low volume fraction reinforcement has been assessed by performing hot compression tests at different temperatures and strain rates. Examination of the obtained stress-strain relationships revealed the correlation between temperature and strain hardening extent. Forming at elevated temperatures enables obvious strain rate hardening and reasonably high ductility of the MMC. The developed unified material model includes evolution of dislocations resulting from plastic deformation, recovery and punching effect due to differential thermal expansion between matrix and reinforcement particles during non-steady state heating and plastic straining. Good agreement has been obtained between experimental and computed results. The proposed material model contributes greatly to a more thorough understanding of flow stress behaviour and microstructural evolution during the hot forming of MMCs.

Keywords: Metal Matrix Composite (MMC), hot compression, AA6061, B_4C, dislocation

1. Introduction

Metal matrix composites (MMC) comprise a relatively wide range of materials defined by composition of matrix and of reinforcement together with its geometry (Kaczmar *et al.*, 2000). Particle-reinforced aluminium alloy/B_4C MMC is a popular candidate in automotive, aerospace and nuclear industries, since boron carbide (B_4C) exhibits very high hardness, relatively low density and good thermal and chemical stability (Guo and Zhang, 2017). Raw MMCs are manufactured today using mostly either particle introduction techniques through liquid-stirring or casting, pressure infiltration or powder metallurgy (Ye and Liu, 2004). The final geometry of MMC parts with a high volume fraction reinforcement is usually obtained by machining. Whereas, a low volume fraction MMCs may be processed by extrusion, drawing or rolling in which the plasticity of the matrix material is exploited. The resultant bar or sheet often requires secondary manufacturing operations to produce the final product geometry. It is advisable to perform

such manufacturing processes on MMCs at elevated temperatures where ductility is higher and forming load is lower (Aour and Mitsak, 2016). This combination increases manufacturing capability and results in an increased material yield compared with machining to achieve final part geometry. Therefore, it is important to characterize the deformation behaviour of MMCs with the low volume fraction of reinforcement under hot working conditions, including mechanisms of deformation and corresponding microstructural evolution.

Significant research has been performed on hot forming of MMCs and related deformation mechanisms. The mechanism of matrix strengthening and microstructure evolution during hot deformation becomes more complicated with the addition of reinforcement particles of different materials, shapes and sizes. Wang *et al.* (2017) found that a dynamic recrystallization (DRX) phenomenon, which depends on temperature and strain rate, was the main softening mechanism when hot compressing AA6061/B_4C composite. Ganesan *et al.* (2004) observed dynamic recrystallization and wedge cracking characterising the hot working of AA6061/15% SiC_p. However, although relative microstructural evolutions were identified, steady flow stress was still modelled phenomenologically using the Zener-Hollomon parameter and the Arrhenius constituent model. The evolution of dislocations associated with hardening was not taken into account. Physically-based models of hot formed MMCs are lacking this phenomenon.

High strength ceramic particles, such as SiC_p, B_4C and ZrB_2, are commonly used to increase MMC strength and thermal stability (Ibrahim *et al.*, 1991). When these MMCs are heated to elevated temperatures, the differential thermal expansion between the particles and matrix alloy can induce dislocation punching (Chawla and Chawla, 2004) during thermal quenching, which is also believed to affect the hardening during deformation. Furthermore, plastic deformation produces temperature increase which can further aggravate dislocation punching. The dominant mechanisms influencing material flow stress behaviour of low volume fraction reinforcement MMCs are punching dislocation and dislocation evolution during deformation of the matrix material, exemplified by plastic strain induced dislocation accumulation and recovery (Lin *et al.*, 2005). Both mechanisms should be included in constitutive models for this type of material.

The objectives of this study are to investigate hot deformation behaviour of MMCs and to further develop a unified physically-based visco-plastic constitutive model for hot forming of discontinuously reinforced MMCs with a low volume fraction of high strength particles. Strengthening mechanisms of discontinuous particle reinforced MMCs are briefly reviewed in this paper, then the development of a visco-plastic material model based on a dislocation evolution mechanism is presented. The feasibility of hot forming of MMCs was proved through hot compression tests. In addition, the constitutive equations of the material model were calibrated using experimentally generated stress-strain relationships. The established model is believed to be the first one ever presented, which is based on the physical mechanisms of particle strengthening and dislocation evolution during hot deformation.

2. Strengthening mechanisms in hot working particle reinforced MMCs

2.1. Modulus

Various methods have been proposed to predict the elastic modulus of composites. Each of the existing models has limits and is unable to cover factors of reinforcement volume fraction, shape, contiguity and distribution. Hashin and Shtrikman (1963) proposed upper and lower bounds for an isotropic aggregate, based on variational principles of linear elasticity. For high volume fraction cases, normally greater than 0.5, Kröner (1958) and Budiansky (1965) proposed a self-consistent methodology to model effective Young's modulus of MMCs with spherical reinforcements. The relationships between Young's modulus E, shear modulus G and bulk modulus K is given in Eq. $(2.1)_1$. On the assumption of an unchanged Poisson's ratio, Young's

modulus can be obtained from shear and bulk modulus. Mura (1987) provided an estimation of the effective moduli for relatively small volume fractions of reinforcing particles, as shown in Eqs. $(2.1)_2$ and $(2.1)_3$. The moduli of a composite are determined by the reinforcement and matrix material for a certain volume percentage of reinforcements. In this theory, the reinforcement geometry is assumed to be spherical. Then, the effective Young's modulus of composite can be obtained from Eq. $(2.1)_1$. It should be noted that the theory was focused on finite concentrations of reinforcements, and the approach is only valid for a relatively small volume fraction of reinforcements, normally less than 0.25

$$\begin{aligned} E &= 2G(1+\nu) = 3K(1-2\nu) \\ G_c &= G_m\Big[1 + V_p(G_m - G_p)\Big/\Big\{G_m + 2(G_p - G_m)\frac{4-5\nu_m}{15(1-\nu_m)}\Big\}\Big]^{-1} \\ K_c &= K_m\Big[1 + V_p(K_m - K_p)\Big/\Big\{K_m + \frac{1}{3}(K_p - K_m)\frac{1+\nu_m}{1-\nu_m}\Big\}\Big]^{-1} \end{aligned} \tag{2.1}$$

where ν is the Poisson's ratio, G is the shear modulus and K is the bulk modulus of the material. G_c, G_m and G_p are the shear modulus of the composite, matrix and reinforcement, respectively. K_c, K_m and K_p are the bulk modulus of the composite, matrix and reinforcement, respectively. ν_c, ν_m and ν_p are the Poisson's ratio of the composite, matrix and reinforcement, respectively. V_p represents the volume fraction of reinforcements.

2.2. Strengthening

2.2.1. Direct strengthening

Direct strengthening is common in continuous fiber-reinforced (Khosoussi *et al.*, 2014) and discontinuously fiber or particle reinforced composites. The main mechanism of direct strengthening is load transfer from the point of application through the low strength matrix to the high strength reinforcement across the matrix/reinforcement interface. Therefore, apparent strengthening results from the additional load carried by the reinforcements. To model such a strengthening phenomenon, Nardone and Prewo (1986) proposed a modified shear-lag model for load transfer in particulate materials. The model incorporates load transfer from the particle ends (which is not applicable to continuous-fiber reinforced composites due to the large aspect ratio). The yield strength of the particulate composite σ_{cy} is increased over the matrix yield strength σ_{my}

$$\sigma_{cy} = \sigma_{my}\Big[V_p\Big(\frac{S+4}{4}\Big) + V_m\Big] \tag{2.2}$$

where S is the aspect ratio of the particle, V_p is the volume fraction of particles, and V_m is the volume fraction of the matrix. The relation shown in Eq. (2.2) does not include effects of particle size and matrix microstructure on the load transfer. Wu *et al.* (2016) investigated the effects of particle size and spatial distribution on the mechanical properties of B_4C reinforced composites. It is demonstrated that for a given volume fraction, reducing the particle size of the B_4C leads to a greater increase in the strength. The contribution of reducing the particle size can be estimated using as

$$\Delta\sigma_d \propto \sqrt{\frac{1}{d}} \tag{2.3}$$

where $\Delta\sigma_d$ represents the increment of the yield strength due to particle size, and d is the average size of particles in the spherical assumption.

2.2.2. Indirect strengthening

Indirect strengthening is believed to be caused by changes of matrix microstructure and properties with the addition of the reinforcement. Thermal expansion mismatch between the reinforcement and matrix alloy can result in a build-up of internal stresses where there is a change in temperature, such as occurs during thermal quenching (Suh *et al.*, 2009). Such a mismatch is a general and important feature of MMCs, especially with the combination of a high coefficient of thermal expansion (CTE) metallic matrix and a low CTE high strength ceramic reinforcement. If the internal stress generated by differential thermal expansion is greater than the yield stress of the matrix, then dislocations form at reinforcement/matrix interfaces and accumulate within a domain surrounding the reinforcement, as shown in Fig. 1. Hence, "thermally induced dislocation

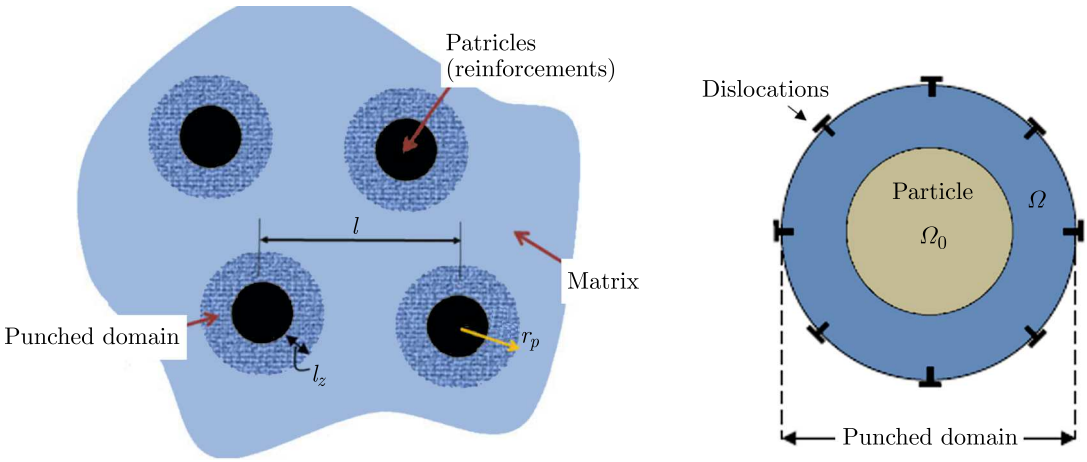

Fig. 1. Schematic of dislocation punching micromechanics (Suh *et al.*, 2009)

punching" results in an indirect strengthening of the matrix. Besides the thermal effects of CTE mismatch during thermal quenching, the internal stress related to differential thermal expansion may also occur if the composite experiences a positive temperature variation under hot forming conditions, such as externally applied heating or temperature rise due to plastic deformation. The matrix domain expands but is constrained by the reinforcements. The matrix material strength is much lower at elevated temperatures, so it is easier for the induced internal stress to exceed the matrix yield strength resulting in dislocations being punched into the matrix. It should be noted that the phenomenon of punched dislocations should be considered only if the heating rate is high and if the soaking time is short. Otherwise, static recovery will eliminate the punched dislocations during the non-steady positive temperature variation. Arsenault and Shi (1986) developed a model to quantify the degree of dislocation punching due to CTE mismatch between a particle and the matrix, schematically shown in Fig. 1. The dislocation density of the punched zone due to differential thermal expansion is given by

$$\rho_{CTE} = \frac{D\varepsilon_{TM}V_p}{b(1-V_p)d} \tag{2.4}$$

where D is a geometric constant, b is the Burgers vector, d is the diameter of the reinforcement particle, and ε_{TM} is the thermal misfit strain, $\varepsilon_{TM} = \Delta\alpha\Delta T$. $\Delta\alpha$ is the difference in the coefficient of thermal expansion between the matrix and reinforcement, and ΔT is the temperature variation. The incremental increase in strength due to dislocation punching can be given as

$$\Delta\sigma_{ind} = \psi G_m b\sqrt{\rho_{CTE}} \tag{2.5}$$

where ψ is a constant. Substituting Eq. (2.4) into Eq. (2.5), the strength increment due to this indirect strengthening mechanism is given by Eq. (2.6) with further consideration of the aspect ratio of the reinforcement particles S

$$\Delta\sigma_{ind} = \psi G_m b \sqrt{\frac{D\varepsilon_{TM} V_p S}{b(1-V_p)d}} \tag{2.6}$$

3. Development of the visco-plastic constitutive model

3.1. Modelling of modulus

The addition of reinforcement particles significantly increases the stiffness of composites compared with that of the matrix alone. For simplicity, Eq. $(2.1)_3$ may be used to represent approximately the relationship between Young's modulus and shear modulus by assuming the Poisson's ratio to be constant. Young's modulus of composites can be also approximated by a formulation shown as

$$E_c = E_m \frac{1 + V_p(E_m - E_p)}{E_m + \delta_1(E_p - E_m)\delta_2} \tag{3.1}$$

where δ_1 and δ_2 are constants. E_c, E_m and E_p are Young's moduli of composite, matrix and reinforcement, respectively.

In order to simplify Eq. (3.1), giving $E_1 = \delta_1\delta_2$, substitute E_1 into Eq. (3.1). Equation (3.1) can be rewritten as follows

$$E_c = E_m \Big[\frac{(1 - E_1 + V_p)E_m + (E_1 - V_p)E_p}{(1 - E_1)E_m + E_1 E_p}\Big]^{-1} \tag{3.2}$$

In terms of hot forming low volume fraction composite materials, in this study, Young's modulus of the matrix metal is considered dependent on bulk temperature, while that of reinforcement particles is considered as constant.

3.2. Modelling punched dislocation density

The dislocation punching feature is determined by temperature variation during hot forming, which can be divided into two parts. Contribution of the first part comes from heating the composite from the room temperature to its forming temperature. The initial dislocation density due to differential thermal expansion is considered to be zero. During heating and according to Eq. (2.4), the rate of punched dislocation density can be expressed as a function of temperature history. Considering the instantaneous heating rate, this becomes as defined in

$$\dot{\rho}_{CTE} = \frac{D\Delta\alpha\Delta\dot{T}V_p}{b(1-V_p)d} \tag{3.3}$$

where $\Delta\dot{T}$ represents the rate of temperature change.

Contribution of the second part results from adiabatic heating during hot working (Bai *et al.* 2013). Adiabatic heating is believed to result from plastic work during hot working (Khan *et al.*, 2004). The temperature increment can be calculated from experimental stress-strain curves using

$$\Delta T = \frac{\eta}{c_m \rho_m} \int_0^{\varepsilon_p} \sigma(\varepsilon_p)\, d\varepsilon_p \tag{3.4}$$

where η represents the fraction of heat dissipation caused by plastic deformation (Khan *et al.*, 2004), c_m and ρ_m are specific heat and mass density of the matrix material, respectively, σ is the instant flow stress and ε_p is the plastic strain. In this study, the variable related to temperature

increase arising from plastic deformation is expressed in terms of a derivative in order to unify the constitutive equations

$$\dot{T}_{\varepsilon} = \eta \frac{\sigma}{c_m \rho_m} |\dot{\varepsilon}_p| \tag{3.5}$$

where T_{ε} is temperature rise due to plastic straining. In ideal isothermal deformation conditions, the instantaneous temperature T is equal to the initial temperature T_0. However, when heat generated due to large plastic deformation cannot be neglected, the instantaneous temperature T equals $(T_0 + \Delta T)$, where ΔT is the temperature rise regarded as a function of the deformation and deformation rate. According to Eq. (3.5), deformation induced temperature increase can be determined through numerical integration based on the stress-strain relationships for a fixed strain rate and stress state. Therefore, substituting Eq. (3.5) into Eq. (3.3), the rate of accumulated dislocation due to thermal expansion mismatch can be rewritten as

$$\dot{\overline{\rho}}_{CTE} = D \frac{V_p}{1 - V_p} \eta \frac{\sigma}{c_m \rho_m} |\dot{\varepsilon}_p| \tag{3.6}$$

3.3. Formulation of constitutive equations

Physically-based visco-plastic constitutive equations have been proposed for the modelling of plastic deformation of many metals, especially in hot forming conditions. The significant contribution of these models is to enable a variety of phenomena to be modelled, including dislocation accumulation and annealing, dynamic recovery and recrystallization, based on the specific deformation mechanisms. Each aspect of microstructural evolution can be treated as a variable in the constitutive equations. These constitutive equations are also suitable for hot working discontinuous particle reinforced MMCs. However, high strength reinforcement adds new mechanisms and effects on the modulus and microstructural evolutions which also need to be considered and modelled. As interactions between different microstructural phenomena exist, it is impossible to express all the physical phenomena active during hot forming by using a single equation. To thoroughly understand their evolution, this study uses a constitutive model based on an advanced dislocation dominated mechanism (Lin and Dean 2005).

A set of unified visco-plastic constitutive equations is established to model the contribution of particles on the modulus and strength, evolution of dislocation, temperature increase due to adiabatic deformation, and rationalise their effects on the steady plastic flow. This developed material model derives from the dislocation evolution during isothermal hot deformation. The relationships between dislocation density and strain hardening and recovery are characterised in this model. Compared to conventional metals, the dislocation density in this model is divided into plastic deformation induced and thermal expansion induced types. For simplification, several assumptions are used in this model, they are (1) dynamic recrystallization of the material during the initial deformation process is not considered for low-volume fraction reinforcement and relatively high strain rates; (2) thermal strain is not taken into account compared with the great total strain; (3) effects of precipitation on dislocation density are not considered. The set of unified viscoplastic constitutive equations for modelling hot deformation of MMCs with low-volume fraction reinforcements is summarised as follows

$$\dot{\varepsilon}_p = \Big(\frac{\sigma - R - k_e}{K}\Big)^{n1} \qquad \dot{R} = \frac{1}{2} B \frac{\dot{\overline{\rho}}}{\sqrt{\overline{\rho}}} \tag{3.7}$$

and

$$\begin{aligned} \dot{\overline{\rho}}_{str} &= A(1 - \overline{\rho}_{str})|\dot{\varepsilon}_p| - C\overline{\rho}_{str}^{n2} \\ \dot{\overline{\rho}} &= \dot{\overline{\rho}}_{str} + \dot{\overline{\rho}}_{CTE} \qquad \sigma = E_c(\varepsilon - \varepsilon_p) \end{aligned} \tag{3.8}$$

The fundamental equations used are Eq. $(3.7)_1$ to Eq. $(3.8)_3$, given above. To make it clear, general description of each equation representing a particular microstructure mechanism is introduced. Details of the form of each equation are given in the literature (Lin and Dean 2005). Equation $(3.7)_1$ represents the traditional power-law of visco-plastic flow formulation (Mohamed *et al.* 2012), k_e represents the initial yield stress of composites and R represents hardening stress due to dislocation evolution. Equation $(3.7)_2$ represents the evolution of material hardening, which is a function of the normalised dislocation density $\overline{\rho}$ defined by $\overline{\rho} = (\rho - \rho_i)/\rho_{max}$, where ρ_i is the initial dislocation density and ρ_{max} is the maximum (saturated) dislocation density. Therefore, the range of $\overline{\rho}$ is between 0 and 1 during the whole process. Unlike hot forming of metals, the dislocation density in this study is divided into two parts; dislocation density evolution of hot straining of the matrix material $\overline{\rho}_{str}$ and punched dislocation density evolution due to differential thermal expansion $\overline{\rho}_{CTE}$ as given in Eq. (3.6). Equation $(3.8)_1$ represents the rate of accumulation of dislocations induced by the plastic deformation, which takes into account deformation and recovery. Equation $(3.8)_2$ represents the sum of dislocation density arising from plastic deformation and punched dislocations, Eq. (3.6), due to the difference of thermal expansion of the matrix and reinforcement. It should be noted that the difference in thermal expansion arises from the temperature increase resulting from plastic deformation, which is different from the applied heating at the initial stage. Equation $(3.8)_3$ is Hook's law for a simple uniaxial state. In this equation set, k_e, K, $n1$, B, A, C and E_c are temperature dependent variables defined in Eqs. (3.9) and (3.10), while $n2$ is temperature independent material constant

$$k_e = k_1 \exp\Big(\frac{Q_k}{R_g T}\Big)(V_p S + V_m)\sqrt{\frac{1}{d}} + k_2\sqrt{\frac{V_p \Delta T}{(1-V_p)d}} \tag{3.9}$$

and

$$\begin{aligned} K &= K_0 \exp\Big(\frac{-Q_K}{R_g T}\Big) \qquad & n1 &= \frac{n1_1}{\dot{\varepsilon}_p^{n1_2}} \exp\Big(\frac{Q_{n1}}{R_g T}\Big) \\ B &= B_0 \exp\Big(\frac{Q_B}{R_g T}\Big) \qquad & A &= A_0 \exp\Big(\frac{Q_A}{R_g T}\Big) \\ C &= C_0 \exp\Big(\frac{-Q_C}{R_g T}\Big) \qquad & E_m &= E_0 \exp\Big(\frac{Q_E}{R_g T}\Big) \end{aligned} \tag{3.10}$$

Equation (3.9) represents the initial yield strength of the MMC considering direct and indirect strengthening of the reinforcement particles, V_p and V_m represent volume fractions of the reinforcement and matrix respectively. ΔT is the temperature increment during rapid heating. Equations (3.9) to (3.10) represent the Arrhenius equations of temperature dependent variables, where Q describes the activation energy for each variable, and R_g is the universal gas constant. All the material constants in Eqs. (3.9) to (3.10) are temperature independent. It should be noted that Young's modulus of MMC is a function of the matrix modulus and particle modulus, which is modelled in the previous Section. Considering the thermal stability of high strength reinforcements, only Young's modulus of the matrix is temperature dependent, defined in Eq. (3.10), while Young's modulus of reinforcements is considered to be a constant.

4. Hot compression tests

4.1. Materials

Experiments have been undertaken using AA6061/B_4C provided by Harbin Institute of Technology. The composite samples were produced with a 15% volume fraction reinforcement using a pressure infiltration method. Single crystal B_4C particles were used having an average particle

size of 17.5 μm (Zhou *et al.* 2014). The bulk composite material was then extruded into circular bars and then machined into standard cylindrical samples with length of 12 mm and diameter of 8 mm. The selection of sample dimensions was chosen so as to avoid inelastic buckling prior to plastic deformation. The matrix material was AA6061. The main chemical compositions of B_4C and AA6061 are given in Tables 1 and 2, respectively.

Table 1. Main chemical composition of B_4C [%]

Element	B	C	Fe	Si	Ca	F
wt [%]	80.0	18.1	1.0	0.5	0.3	0.025

Table 2. Main chemical composition of AA6061 [%]

Element	Fe	Si	Mn	Cr	Mg	Zn	Al
wt [%]	0.70	0.80	0.15	0.35	1.2	0.25	Remain

4.2. Experimental set-up and test programme

High temperature uniaxial compression tests were performed using the thermo-mechanical simulator Gleeble 3800. Specimens were heated at a pre-determined heating rate by resistance heating, and temperature was precisely controlled by feedback from a thermocouple welded to the middle of the specimen. Graphite foil and high-temperature graphite paste were used at the interfaces between the specimen and Gleeble anvils to reduce interfacial friction and obtain a more uniform deformation. Strain was measured using a C-gauge which detected a change in the specimen diameter. The experimental set-up is shown in Fig. 2.

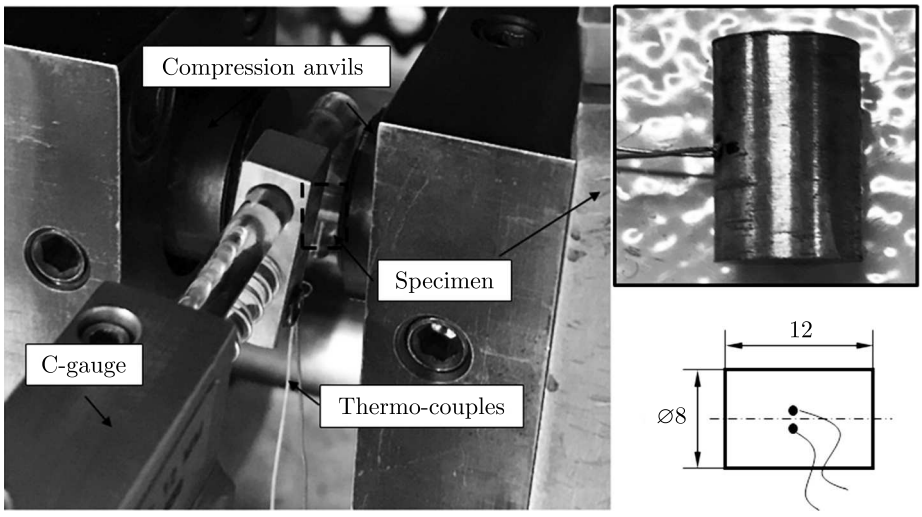

Fig. 2. Experimental set-up for hot compression test (all dimensions are in mm)

Figure 3 shows the temperature profile of a specimen in the hot compression test. A two-stage heating strategy was utilised to obtain a uniform temperature and to avoid overshoot. Initially, the specimen was heated up at a rate of 5°C/s to 50°C below the specified target deformation temperature. Then, it was further heated to the target temperature at a rate of 2.5°C/s. After soaking for 1 min, the specimen was uniaxially hot compressed at different strain rates. In this study, the temperatures selected were 350°C, 400°C, 450°C. The strain rates used were 0.01 s^{-1}, 0.1 s^{-1} and 1 s^{-1}.

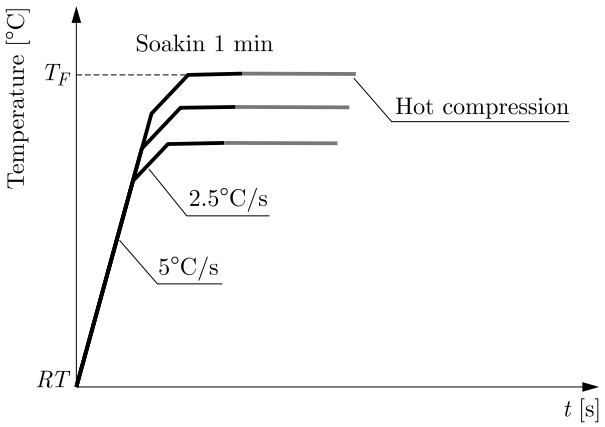

Fig. 3. Temperature profile of the hot compression test

5. Results and discussion

5.1. Determination of constitutive equations

The experimental results from hot compression tests were used to determine material constants in the developed constitutive relationships. Firstly, according to Eqs. (3.2), (3.9) and (3.10), Young's modulus and the initial yield strength of the composite vary with the temperature from the applied heat, and are also significantly greater than those of the matrix. Figure 4 shows the similarity between the equation fitted and experimentally determined values. Good agreement exists between the fitted curves and experimental results. Differences that exist are believed to be due to the difficulty in determining accurate values from hot compression results, considering the slopes of the modulus are very sharp. Table 3 gives the material properties of the matrix alloy and reinforcement particles at room temperature. Tables 4 lists values of material constants used for calculating the strength variables.

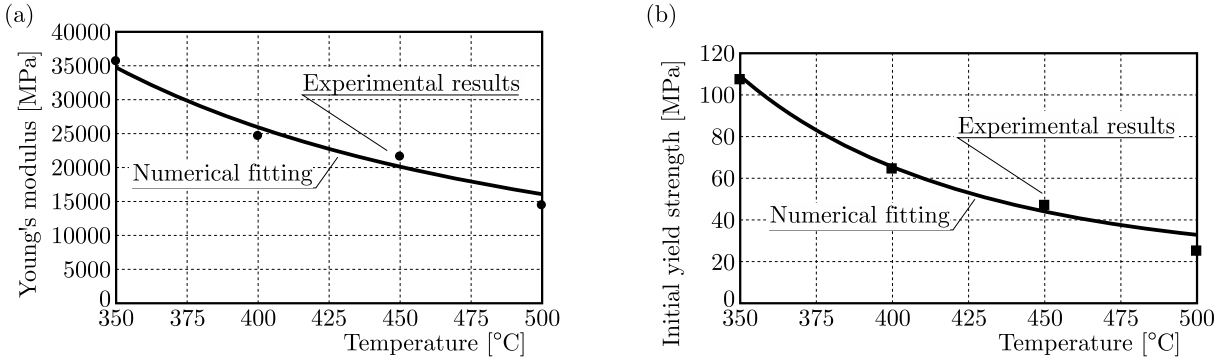

Fig. 4. Comparisons of numerical fitting (solid lines) and experimental results (solid symbols) of strength variables, where (a) Young's modulus and (b) initial yield strength

Table 3. Material properties of the matrix alloy and reinforcement

V_p	V_m	d [μm]	E_p [MPa]	η	c_m [J/(kg K)]	ρ_m [kg/m^3]
0.15	0.85	17.5	362000	0.9	890	2700

Other material constants in the dominant equation set were determined using a combination of Evolutionary Programming (EP) optimisation techniques (Li *et al.*, 2002) as well as trial and

Table 4. Determined constants for Young's modulus and initial yield strength

E_0	Q_E	E_1	k_1	Q_k	k_2
590	20140	0.67	0.0017	40950	0.075

error methodology. The explanation of the optimisation method and description of numerical procedures for determining the material constants of constitutive equations are described by Cao and Lin (2008). Table 5 shows the determined material constants of Eqs. $(3.10)_{1\text{-}5}$.

Table 5. Determined constants for material constants

K_0	B_0	C_0	A_0	$n1_1$	$n1_2$
326.5	0.2774	114.9	0.144	0.04691	−0.4111
Q_K	Q_B	Q_C	Q_A	Q_{n1}	$n2$
9634	21780	51760	18420	29760	1

5.2. Comparison of experimental results and the constitutive model

Figures 5 and 6 show comparisons between the Gleeble experimental results (symbols) and the modelling results (solid lines). Three typical hot forming temperatures 350°C, 400°C and 450°C and three different strain rates from $0.01\,\mathrm{s}^{-1}$ to $1\,\mathrm{s}^{-1}$ were chosen. As can be seen in both figures, good fitting accuracy was obtained. Dynamic recrystallization at the beginning of deformation which results in the strain softening is neglected in the current model for simplicity of numerical fitting. Figure 5 shows that MMC stress level reduces with the increasing forming temperature, and is lower than that at the room temperature (Chen *et al.*, 2015). When the

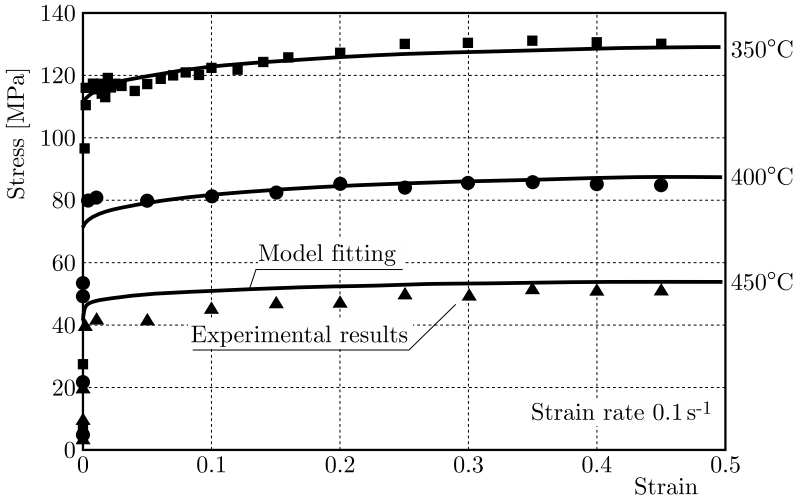

Fig. 5. Comparison of stress-strain relationships from hot compression tests at different temperatures and a strain rate of $0.1\,\mathrm{s}^{-1}$. Symbols represent experimental results and solid lines are computed predictions from the model

composite was compressed at higher temperatures, such as 450°C and lower strain rates, such as $0.01\,\mathrm{s}^{-1}$, the stress level exhibited a plateau. The absence of strain hardening is believed to be beneficial for bulk forming, such as extrusion and forging, as the strain hardening would increase the forming load significantly and may cause cracks of the forming dies. In addition, the extent of strain hardening increased with the decreasing temperature at a fixed strain rate, considering dislocation recovery was not significant and visco-plastic feature was not obvious. The diffusion process was not sufficient at lower temperatures. Moreover, compared with forming at the room

temperature, an increased strain limit without crack was observed representing a reasonable ductility improvement, which enhanced the feasibility of hot forming MMCs. For temperature 400°C, a clear strain rate effect was also observed in the hardening curves. With increasing strain rate, the stress level increased, as shown in Fig. 6. In summary, higher temperatures and lower strain rates are recommended for hot bulk forming the low volume MMC materials.

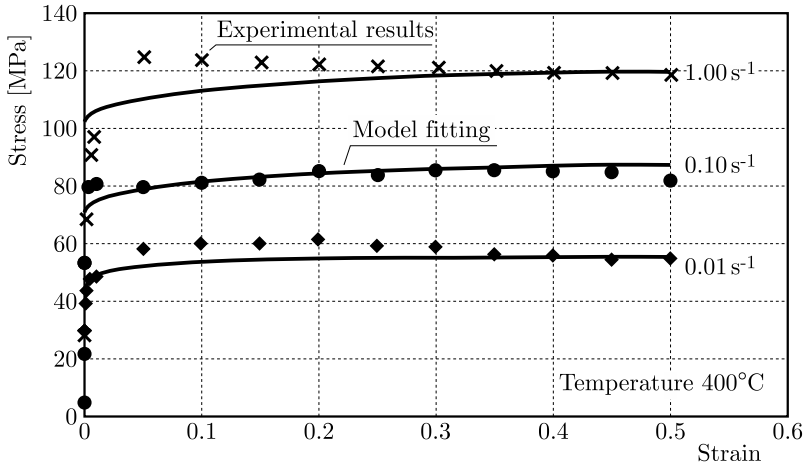

Fig. 6. Comparison of stress-strain relationships from hot compression tests at different strain rates and temperature of 400°C. Symbols represent experimental results and solid lines are computed predictions from the model

6. Conclusions

It is concluded that hot forming processes can be used to shape MMCs with a low volume fraction of reinforcements. Stress-strain relationships obtained from hot compression tests of AA6061/15% B_4C MMC show that strain hardening is only obvious at relatively low temperatures, and the flow stress and the flow stress remains relatively constant at higher temperatures, which is believed to be beneficial for bulk forming. The strain rate hardening is also significant at high temperatures dominated by the visco-plastic mechanism. In addition, the first ever unified physically-based visco-plastic material model has been developed for hot forming of low volume fraction reinforcement MMCs. The evolution of dislocations has been modelled taking into account the effects of temperature history and plastic deformation. This material model, suitable for finite element simulations, can be further extended to predict stress-strain relationships of MMCs under different process conditions.

Acknowledgements

The research in this paper was funded by the European Union's Horizon 2020 research and innovation programme under Grant Agreement No. 723517 as a part of the project "Low Cost Materials Processing Technologies for Mass Production of Lightweight Vehicles (LoCoMaTech)".

References

1. Aour B., Mitsak A., 2016, Analysis of plastic deformation of semi-crystalline polymers during ECAE process using 135° die, *Journal of Theoretical and Applied Mechanics*, **54**, 1, 263-275, DOI:10.15632/jtam-pl.54.1.263
2. Arsenault R.J., Shi N., 1986, Dislocation generation due to differences between the coefficients of thermal expansion, *Materials Science and Engineering*, **81**, 175-187. DOI: 10.1016/0025--5416(86)90261-2

3. Bai Q., Lin J., Dean T.A., Balint D.S., Gao T., Zhang Z., 2013, Modelling of dominant softening mechanisms for Ti-6Al-4V in steady state hot forming conditions, *Materials Science and Engineering A*, **559**, 352-358 DOI: 10.1016/j.msea.2012.08.110

4. Budiansky, B., 1965, On the elastic moduli of some heterogeneous materials, *Journal of the Mechanics and Physics of Solids*, **13**, 4, 223-227, DOI: 10.1016/0022-5096(65)90011-6

5. Cao J., Lin J., 2008, A study on formulation of objective functions for determining material model, *International Journal of Mechanical Sciences*, **50**, 2, 193-204, DOI: 10.1016/j.ijmecsci.2007.07.003

6. Chawla K.K., Chawla N., 2004, Metal-matrix composites, *Material Science and Technology*, **1**, 1-25, DOI: 10.1016/B978-0-08-050073-7.50011-7

7. Chen H.S., Wang W.X., Li Y. Li, Zhang P., Nie H.H., Wu Q.C., 2015, The design, microstructure and tensile properties of B_4C particulate reinforced 6061Al neutron absorber composites, *Journal of Alloys and Compounds*, **632**, 23-29, DOI: 10.1016/j.jallcom.2015.01.048

8. Ganesan G., Raghukandan K., Karthikeyan R., Pai B.C., 2004, Development of processing maps for 6061 Al/15% SiC_p composite material, *Materials Science and Engineering A*, **369**, 1-2, 230-235, DOI: 10.1016/j.msea.2003.11.019

9. Guo H., Zhang Z., 2017, Processing and strengthening mechanisms of boron-carbide-reinforced aluminum matrix composites, *Metal Powder Report*, DOI: 10.1016/j.mprp.2017.06.072

10. Hashin Z., Shtrikman S., 1963, A variational approach to the theory of the elastic behaviour of multiphase materials, *Journal of the Mechanics and Physics of Solids*, **11**, 2, 127-140, DOI: 10.1016/0022-5096(63)90060-7

11. Ibrahim I.A., Mohamed F.A., Lavernia E.J., 1991, Particulate reinforced metal matrix composites – a review, *Journal of Materials Science*, **26**, 5, 1137-1156, DOI: 10.1007/BF00544448

12. Kaczmar J.W., Pietrzak K., Wlosinski W., 2000, The production and application of metal matrix composite materials, *Journal of Materials Processing Technology*, **106**, 1-3, 58-67, DOI: 10.1016/S0924-0136(00)00639-7

13. Khan A.S., Suh Y.S., Kazmi R., 2004, Quasi-static and dynamic loading responses and constitutive modeling of titanium alloys, *International Journal of Plasticity*, **20**, 12, 2233-2248, DOI: 10.1016/j.ijplas.2003.06.005

14. Khosoussi S., Mondali M., Abedian A., 2014, An analytical study on the elastic-plastic behavior of metal matrix composites under tensile loading, *Journal of Theoretical and Applied Mechanics*, **52**, 2, 323-334

15. Kröner E., 1958, Berechnung der elastischen Konstanten des Vielkristalls aus den Konstanten des Einkristalls, *Zeitschrift für Physik*, **151**, 4, 504-518, DOI: 10.1007/BF01337948

16. Li B., Lin J., Yao X., 2002, A novel evolutionary algorithm for determining unified creep damage constitutive equations, *International Journal of Mechanical Sciences*, **44**, 5, 987-1002, DOI: https://doi.org/10.1016/S0020-7403(02)00021-8

17. Lin J., Dean T.A., 2005, Modelling of microstructure evolution in hot forming using unified constitutive equations, *Journal of Materials Processing Technology*, **167**, 2-3, 354-362, DOI: 10.1016/j.jmatprotec.2005.06.026

18. Lin J., Liu Y., Farrugia D.C.J., Zhou M., 2005, Development of dislocation-based unified material model for simulating microstructure evolution in multipass hot rolling, *Philosophical Magazine*, **85**, 18, 1967-1987, DOI: 10.1080/14786430412331305285

19. Mohamed M.S., Foster A.D., Lin J., Balint D.S., Dean T.A., 2012, Investigation of deformation and failure features in hot stamping of AA6082: Experimentation and modelling, *International Journal of Machine Tools and Manufacture*, **53**, 1, 27-38, DOI: 10.1016/j.ijmachtools.2011.07.005

20. Mura T., 1987, *Micromechanics of Defects in Solids*, Springer, ISBN 978-94-009-3489-4

21. Nardone V.C., Prewo K.M., 1986, On the strength of discontinuous silicon carbide reinforced aluminum composites, *Scripta Metallurgica*, **20**, 1, 43-48, DOI: 10.1016/0036-9748(86)90210-3

22. Suh Y.S., Joshi S.P., Ramesh K.T., 2009, An enhanced continuum model for size-dependent strengthening and failure of particle-reinforced composites, *Acta Materialia*, **57**, 19, 5848-5861, DOI: 10.1016/j.actamat.2009.08.010

23. Wang K.K., Li X.P., Li Q.L., Shu G.G., Tang G.Y., 2017, Hot deformation behavior and microstructural evolution of particulate-reinforced AA6061/B_4C composite during compression at elevated temperature, *Materials Science and Engineering A*, **696**, 1, 248-256, DOI: 10.1016/j.msea.2017.03.013

24. Wu C.D., Ma K.K., Wu J.L., Fang P., Luo G.Q., Chen F., Shen Q., Zhang L.M., Schoenung J.M., Lavernia E.J., 2016, Influence of particle size and spatial distribution of B_4C reinforcement on the microstructure and mechanical behavior of precipitation strengthened Al alloy matrix composites, *Materials Science and Engineering A*, **675**, 421-430, DOI: 10.1016/j.msea.2016.08.062

25. Ye H.Z., Liu X.Y., 2004, Review of recent studies in magnesium matrix composites, *Journal of Materials Science*, **39**, 20, 6153-6171, DOI: 10.1023/B:JMSC.0000043583.47148.31

26. Zhou Z.S., Wu G.H., Jiang L.T., Li R.F., Xu Z.G., 2014, Analysis of morphology and microstructure of B_4C/2024Al composites after 7.62 mm ballistic impact, *Materials and Design*, **63**, 658-663, DOI: 10.1016/j.matdes.2014.06.042

Manuscript received January 5, 2018; accepted for print February 7, 2018